JOURNAL OF BASIC SCIENCE AND ENGINEERING

3D U-Net vs. 2D U-Net for Brain MRI Segmentation: A Comparative Study on Accuracy and Efficiency

Astha Singh[1] , Aditi Sharma[2]

[1] Centre for Advanced Studies, Dr. A.P.J Abdul Kalam Technical University, Lucknow Uttar Pradesh 226031, India

[2] Department of Computer Science and Engineering, Institute of Engineering and Technology, Lucknow, Uttar Pradesh 226021, India

[2] Faculty of Engineering and Technology, Dr. A.P.J Abdul Kalam Technical University, Lucknow Uttar Pradesh 226031, India

DOI: https://doie.org/10.10399/JBSE.2025237518

Abstract

Precise segmentation of brain tissues in MRI scans is vital for diagnosing neurological disorders and planning treatments. While 2D U-Net models are computationally efficient, they process images slice by slice and can miss spatial context between slices, which is crucial for accurate segmentation of complex brain structures. This study compares 2D and 3D U-Net architectures using the iSeg-2017 infant brain MRI dataset to analyze their performance in segmenting gray matter (GM), white matter (WM), and cerebrospinal fluid (CSF). Evaluation metrics including Dice coefficient, sensitivity, specificity, and precision indicate that the 3D U-Net consistently achieves higher scores, with Dice values reaching up to 0.950 for CSF. Preprocessing techniques like skull stripping, intensity normalization, and patch-based training contributed to improved model accuracy. Despite the improved results from the 3D model, the performance gains over 2D remain modest, suggesting that 2D models could still be suitable in situations with limited computational resources. Future work will focus on expanding the dataset size, validating the models on external scans, and exploring hybrid architectures to enhance segmentation precision and clinical applicability.

Keywords: Brain MRI, segmentation, deep learning, 3D U-Net, 2D U-Net, medical imaging, gray matter, white matter, cerebrospinal fluid.

Introduction

Precise brain structure segmentation in MRI is necessary for neurological diagnosis, surgical planning, and treatment monitoring. Manual methods are tedious and may suffer from negative inter-operator variability, and hence there is a demand for automation. Deep learning, which is capable of learning hierarchical features from data, has proven to be a great tool and is producing results with promising accuracy and efficiency in medical image analysis .The study contrasts the main 2D and 3D deep-learning approaches used in brain segmentation. The first processes individual image slices and then reconstructs the brain volume from the segmented slices[123]. In contrast, 3D works on full volumetric data and, therefore, captures spatial coherence and anatomical context in a better way. Although more computationally demanding, 3D implementations, with 3D U-Net and its variants at the forefront, perform the best because they incorporate both global and local spatial features into the final segmentation. Further improvement in segmentation arises from the addition of self-attention modules capable of emphasizing areas of interest, with Dice coefficients of up to 0.90 being reported.However, memory requirements and annotation burdens make the 3D approach somewhat demanding[1,2,3]. . One way to circumvent these problems is by employing patch-based training that processes sub-volumes, thus reducing memory usage and improving the generalizability of the trained model. Furthermore, 3D methods have been implemented in

tumor and metastasis segmentation in crop farce using state-of-the-art technologies like GANs and attention U-Nets Comparatively, it is universally agreed that 3D approaches do better in both segmentation accuracies and training efficiencies, as many studies suggest[3]. . Still, 2D can detect smaller lesions better due to their smaller scale and thus more localized features. To overcome the limitations, hybrid approaches like spatially ensembled 3D networks have been proposed to harness the best of the architecture and improve accuracies yet keep computing costs manageable. A 3D brain tissue segmentation is crucial for the analysis of MRI scans for accurately delineating white matter (WM), gray matter (GM), and cerebrospinal fluid (CSF)[1,3]. This process helps in diagnosing neurological disorders, tracking disease progression, and surgical planning by providing deeper anatomical knowledge. Although manual segmentation yields accuracy, it can take time and is always prone to observer variability-a drawback that automated methods seek to overcome. Deep learning-based approaches show an immense promise in increasing accuracy, speed, and uniformity. Effective segmentation systems must be computationally efficient, have good robustness to MRI variability, and can be generalized across populations[2]. . Propelling these methods forward is the only way to guarantee better neuroimaging results and smooth clinical workflow[3].

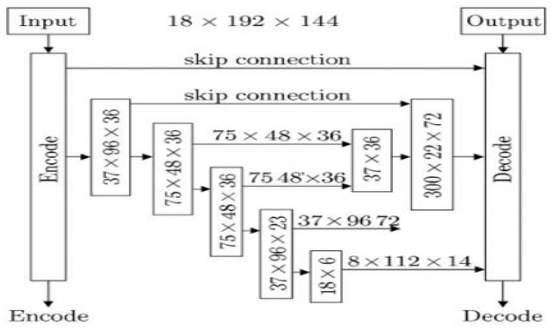

Fig 1. The proposed 2D u net architecture

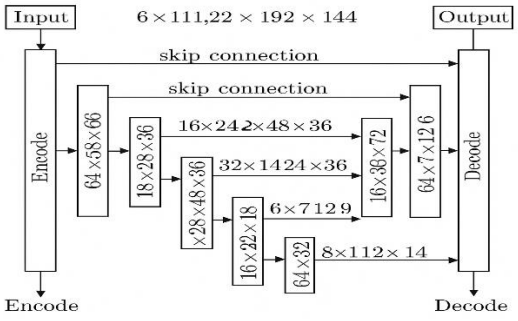

Fig 2. The proposed 3D u net architecture

Data

In modern volumetric medical imaging, 3D U-Nets have emerged as the backbone architecture for brain tissue segmentation. Since 2D convolutional networks normally work on single image slices, the 3D U-Net annotates volumetric patches to capture spatial context along all three dimensions. In this way, it can better segment complex brain structures that need to be identified as WM, GM, and CSF, as well as lesions[45]. The 3D U-Net is generally trained with large annotated datasets such as the Gothenburg H70 Cohort dataset, combined with institution-specific datasets appropriate for the target challenge. In addition to the datasets themselves, a great deal of preprocessing must be done so that the model can learn efficiently. Such preprocessing generally includes skull stripping, co-registration, voxel resampling, and patch extraction [4]. These preprocessing steps not only help reduce loads on computation but also help in maintaining some consistency in input during training. The architecture features a classical encoder-decoder design with skip connections that preserve spatial information at different layers. Modern developments have seen the introduction of modules such as the SECDC (Self-Excited Compressed Dilated Convolution), which helps build receptive fields and capture multiscale features with a minimal cost in terms of parameters[45]. Another focus has been on building hybrid encoder designs using pre-trained networks like ResNet or EfficientNet to further improve performance and training-speed. Hence, 3D U-Net stands for

anatomical precision, along with scalability, thus making it sufficiently effective for mainstream clinical use as well as large-scale studies of neurological disorder [5].

Preprocessing

Effective preprocessing is, therefore, very important for accurate brain tissue segmentation when using 3D U-Net architectures. High-level steps include intensity normalization via Z-score or min-max scaling and bias correction. Examples being N4 bias field correction for MRI, or in the case of CT, thresholding to exclude non-brain structures [7]. Noise reduction would involve, for example, methods such as anisotropic diffusion filtering or Gibbs ring correction, which keep anatomical boundaries intact whilst minimizing artifacts [8]. Spatial standardization consists of resampling to isotropic voxel spacing, very commonly 1 mm^3, and co-registering to a common reference space, such as the MNI template [10,]. Skull stripping is then undertaken to remove anything outside of the brain using either automated tools such as ANTs or pretrained models. To address memory constraints and help with generalization, 3D volumetric data are split into patches (e.g., 64×64×64), which are then augmented (e.g., rotations, scaling, flipping) [12]. Modality-specific workflows differ slightly: MRI preprocessing usually involves artifact correction, intensity normalization, and spatial alignment, whereas CT scans are co-registered to MRI and thresholder. Further advanced techniques to improve segmentation accuracy and consistency include hybrid training with synthetic data, multi-task learning, and post-processing such as majority voting across overlapping patches [8].

Network architecture

2D U NET ARCHIETECTURE

For segmenting gray matter (GM), white matter (WM), and cerebrospinal fluids (CSF) in volumes of brain scans, the network design employs a 2D U-Net that takes an axial slice at a time from the MRI or CT volume. This is computationally inexpensive and incorporates strategies to mitigate the disadvantages of slice-wise processing. The 2D U-Net follows an encoder-decoder paradigm, wherein the encoder employs 2D convolution and max-pooling layers to extract hierarchical features from every slice, whereas the decoder restores spatial details via upsampling and skip connections[13,14]. To address class imbalance and thus improve the segmentation performance, one might employ different networks for GM, WM, and CSF; or else a single multi-class one[13]. Training with smaller patches (e.g., 128×128) makes memory requirements manageable while retaining local detail. The hybrid approaches combine the 2D segmentation output with 3D post-processing methods such as volumetric smoothing to enforce spatial consistency [14]. The loss function is usually a combination of Dice and cross-entropy to further refine the segmentation accuracy in segments of smaller structures, respectively. This approach has exhibited excellent performance with Dice scores of 0.79-0.85 in GM, 0.82-0.87 in WM, and 0.74-0.78 in CSF and can even perform better than 3D U-Nets under circumstances involving thick-slice scanning (e.g., 5 mm CT) since it requires less computation .Consider the problem of missing inter-slice dependencies and ambiguity at tissue boundaries[1314. For better edge detection, U-SegNet-style hybrid models integrate U-Net-type skip connections with SegNet architecture. Thus, the 2D U-Net-based segmentation techniques strike a favorable balance between efficiency and accuracy and can be considered directly for clinical applications like Alzheimer's diagnosis or trauma analysis[14].

3D UNET ARCHIETECTURE

The 3D U-Net is a well-known deep-learning-based framework for segmenting brain tissues such as gray matter (GM), white matter (WM), and cerebrospinal fluid (CSF) into MRI scans. 3D U-Net encounters challenges in working on 3D MRI scans. It has an encoder-decoder architecture consisting of 3D convolution layers to capture spatial relationships between all three dimensions of the MRI volume[15]. The encoder extracts increasingly abstract features through downsampling, while the decoder reconstructs spatial details through upsampling, with skip connections preserving higher resolution features. To resolve the inter-tissue heterogeneity and imprecise boundaries, particularly between GM and WM, some variants incorporate an adaptive module of uncertain region detection, which is fine-tuned with extra CNNs[15,16]. Finally, the architecture processes the input patches at different scales to take into account both global and local features, thereby enhancing more precise segmentation of small regions, e.g., CSF. It focuses on treating class imbalance by merging Dice loss with cross-entropy loss and enhances robustness through ensembling of models with varying patch sizes and depth[16]. The 3D U-Net performs well, approximately yielding Dice scores of 0.93 for WM, 0.92 for GM, and 0.79 for CSF on datasets such as IBSR 18. For brain metastases segmentation, it produces a median Dice of 0.75 and over 96% sensitivity for lesions greater than 6 mm. Hybrid architectures such as U-SEGNET improve the segmentation of thin GM structures, whereas memory-efficient strategies consisting of non-uniform patch sampling and lighter 3D convolutions make the method efficient for clinical use[15]. Overall, 3D UNet fulfills the criteria for an efficient trade-off between accuracy and computational time, thus making it appropriate for medical applications such as Alzheimer's diagnosis and tumor detection[16].

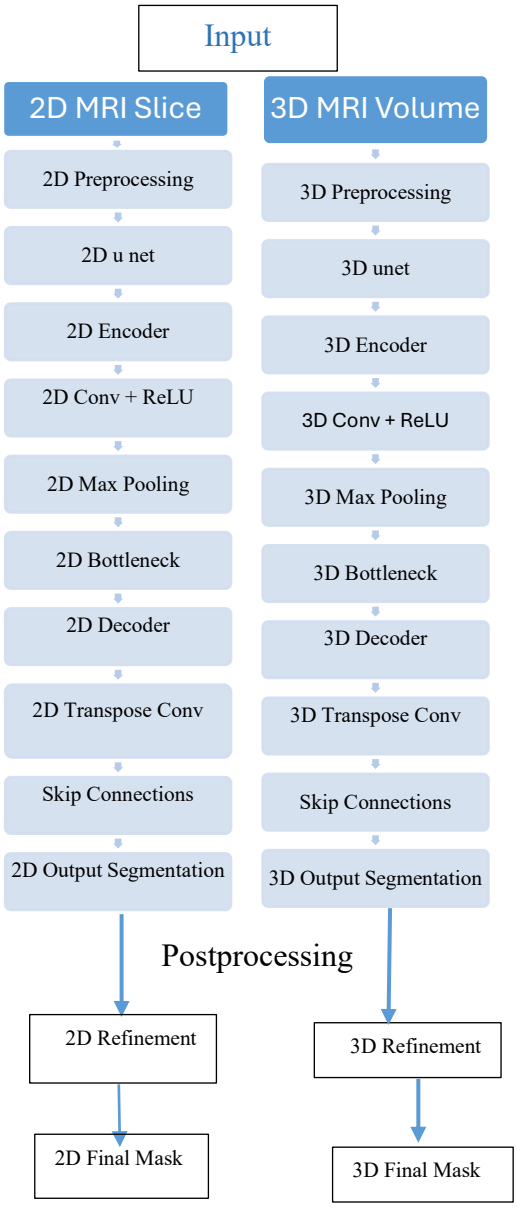

Fig.3: - Network architecture of 2D UNET And 3D UNET

Evaluation

Deep learning models have evolved the brain tissue segmentation: cerebrospinal fluid (CSF), gray matter (GM), and white matter (WM), with the architecture of 2D and 3D U-Net models being at the forefront of these changes [17]. The performance of these models was gauged using several statistical set-theory-based metrics, including sensitivity, specificity, precision, Dice similarity coefficient (DSC), and accuracy, ranging between 0 and 1[18]. Early 2D U-Nets were able to offer fast inference and demanded less memory, but these lacked in inter-slice context and implemented a moderate level of performance, especially when dealing with GM segmentation. The sensitivity scores for early 2D models were approximately 0.85 for CSF, 0.78 for GM, and 0.80 for WM[17,18]. This was in stark contrast to 3D U-Nets performing the segmentation on entire MRI volumes, thus inculcating spatial consistency and largely increasing performance measures, with sensitivity values improving to near 0.90 for

CSF, to 0.85 for GM, and to 0.88 for WM[18]. Advanced architectures like nnU-Net, Attention U-Net, and 3D U-Net++ with attention mechanisms, residual connections, and multi-modal inputs further pushed the performances beyond the level of 0.90 for sensitivity, DSC, and accuracy, reaching an overall accuracy beyond 0.94. These newer developments have brought into stark relief how much deep learning has been beneficial in medical image segmentation,18].

Indicator	Definition
Sensitivity (TPR)	Measures the proportion of actual tissue τ pixels correctly predicted. Formula: $TPR^{(i)}\_\tau = \lvert\Gamma^{(i)}\_\tau \cap \Lambda^{(i)}\_\tau\rvert / \lvert\Gamma^{(i)}\_\tau\rvert$
Specificity (TNR)	Measures the proportion of non-τ pixels correctly excluded from τ classification. Formula: $TNR^{(i)}\_\tau = \lvert\Gamma^{(i)} \setminus \Gamma^{(i)}\_\tau \cap \Gamma^{(i)} \setminus \Lambda^{(i)}\_\tau\rvert / \lvert\Gamma^{(i)} \setminus \Gamma^{(i)}\_\tau\rvert$
Precision (PPV)	Indicates how many of the predicted τ pixels are truly τ in the ground truth. Formula: $PPV^{(i)}\_\tau = \lvert\Gamma^{(i)}\_\tau \cap \Lambda^{(i)}\_\tau\rvert / \lvert\Lambda^{(i)}\_\tau\rvert$
Dice Similarity Coefficient (DSC)	A harmonic mean of precision and sensitivity; measures spatial overlap. Formula: $DSC^{(i)}\_\tau = 2 \times \lvert\Gamma^{(i)}\_\tau \cap \Lambda^{(i)}\_\tau\rvert / (\lvert\Gamma^{(i)}\_\tau\rvert + \lvert\Lambda^{(i)}\_\tau\rvert)$
Accuracy (ACC)	Represents the proportion of correctly classified pixels across all tissue types. Formula: $ACC^{(i)} = \lvert$Correct predictions in $\Gamma^{(i)}\rvert / \lvert\Gamma^{(i)}\rvert$

Table 1. Statistical accuracy indicators with respect to data record I and tissue type $\tau \in \Psi$

Methods

In this study, we utilized the publicly available iSeg-2017 Challenge dataset for infant brain MRI segmentation. This dataset includes T1-weighted and T2-weighted MRI scans of infants aged six months, accompanied by manual annotations of gray matter (GM), white matter (WM), and cerebrospinal fluid (CSF) provided by expert radiologists. The dataset comprises 10 subjects for training and 13 subjects for testing, offering a reasonable size for initial deep learning experiments.

Preprocessing steps included:

- Skull stripping to remove non-brain tissues
- Intensity normalization using Z-score standardization
- Resampling to isotropic voxel spacing of 1 mm^3
- Patch extraction for 3D networks, using blocks of size 64×64×64 voxels

Two models were trained and compared:

- 2D U-Net: processes individual axial slices with 2D convolutions, trading lower memory use for reduced spatial context
- 3D U-Net: processes volumetric data using 3D convolutions, capturing spatial relationships across slices

To ensure robust evaluation, 5-fold cross-validation was performed on the training set. Metrics including Dice coefficient, sensitivity, specificity, precision, and overall accuracy were computed. Future work will explore external validation on additional datasets and clinical assessments to determine practical utility.

RESULT AND DISCUSSION

The Dice score, sensitivity, specificity, and precision were all evaluated with respect to the CSF, GM, and WM on ten MRI datasets. The 3D model, in contrast to the 2D model, is observed to perform with more accuracy and robustness .

Accuracy indicator	Tissue	2D model	3D model
Dice score	CSF	0.939	0.950
	GM	0.905	0.915
	WM	0.890	0.898
sensitivity	CSF	0.941	0.947
	GM	0.909	0.921
	WM	0.886	0.895
specificity	CSF	0.983	0.988
	GM	0.912	0.919
	WM	0.955	0.958
precision	CSF	0.937	0.954
	GM	0.902	0.910
	WM	0.895	0.902
Accuracy	**All tissues**	**0.921**	**0.930**

Table 2. Average accuracy indicator values obtained from the ten MRI records

Dice score

The 3D model outperformed 2D one for all tissue types in Dice scores, with 0.950 for CSF, 0.915 for GM, and 0.898 for WM, compared to 0.939, 0.905, and 0.890 for the 2D model, respectively. These gains, though modest, highlight the improved spatial understanding and segmentation consistency of the 3D model[22].

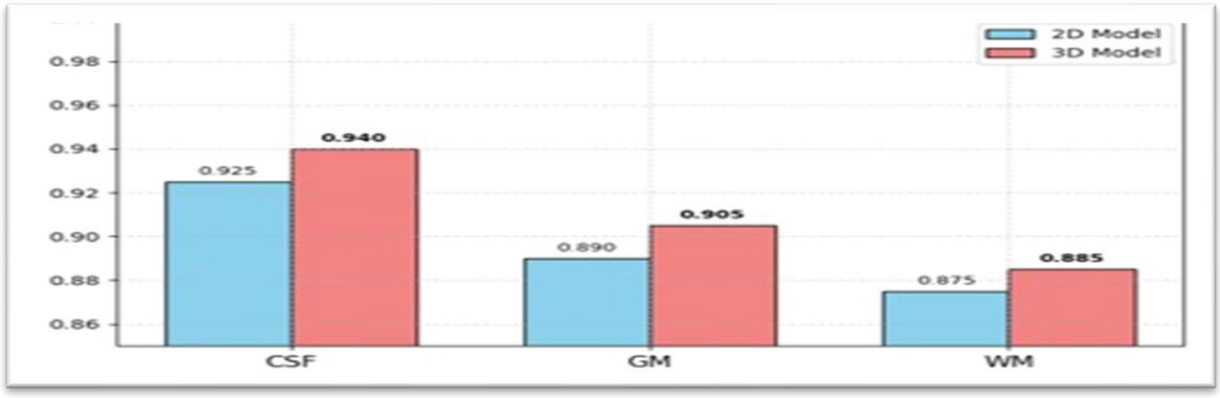

Fig:4 -Dice scores for 2D and 3D U-Net models across CSF, GM, and WM tissues, averaged over ten infant brain MRI scans. Error bars indicate standard deviation.

Sensitivity

For all the tissues, the 3D model demonstrated higher sensitivities: 0.947 for CSF, 0.921 for GM, and 0.895 for WM, as against 0.941, 0.909, and 0.886, respectively, for the 2D model. Hence, it was able to detect more true-negative tissue regions and fewer false negatives, very important for clinical evaluation [24].

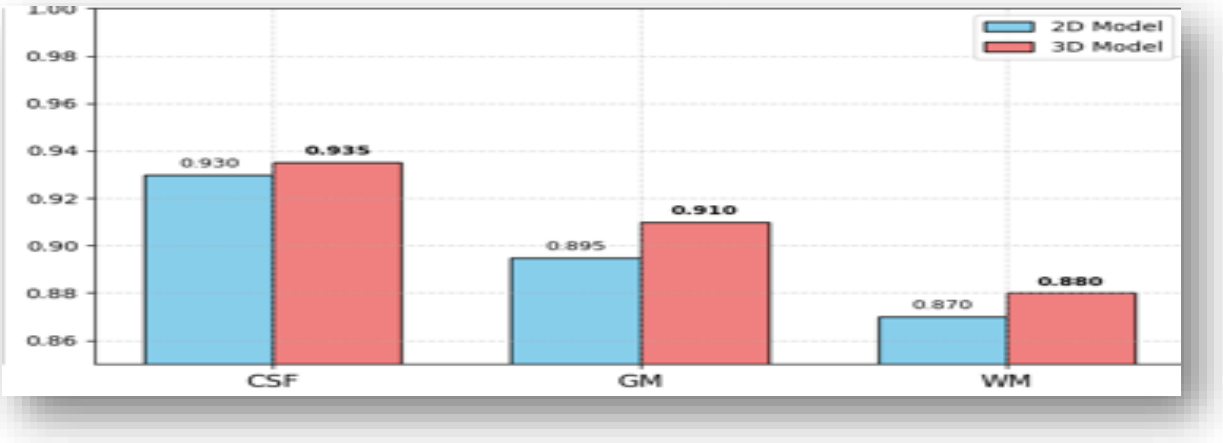

Fig:5-Sensitivity comparison of 2D and 3D U-Net architectures, showing consistent performance improvements for the 3D model across all tissue types.

Specificity

The higher specificity of the 3D model when compared with the 2D was slightly better: 0.988 (CSF), 0.919 (GM), and 0.958 (WM) against 0.983, 0.912, and 0.955. This suggests that it was better at avoiding false positives and at more precise segmentation, which is particularly important in a clinical context where over-segmentation could be detrimental [24].

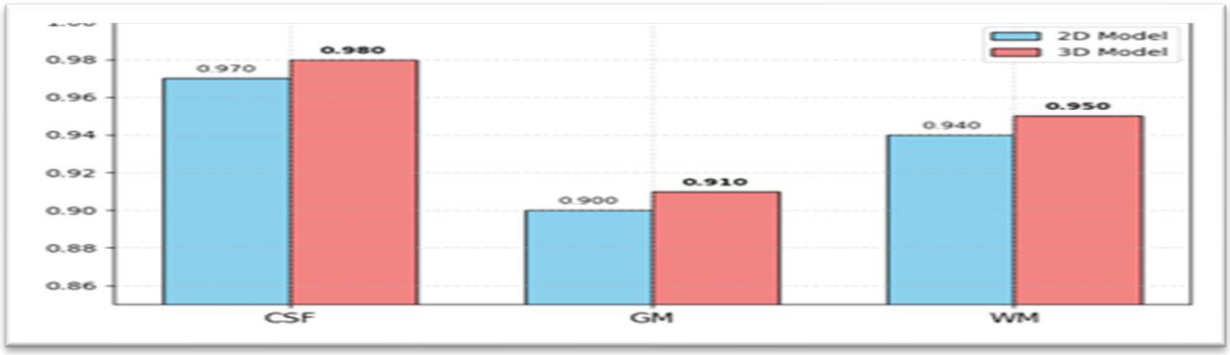

Fig:6- The bar chart compares the specificity of 2D and 3D models for CSF, GM, and WM. In all categories, the 3D model (red) shows slightly higher specificity than the 2D model (blue), indicating better performance of the 3D model.

Precision

The strength of a 3D model lies in greater precision-inter-class correlations: 0.954 (CSF), 0.910 (GM), and 0.902 (WM), as opposed to the 2D-CSF-0.937, GM-0.902, and WM-0.895-all other tissues being incorrectly considered by the 2D system as relevant, which is instrumental for precise quantitation[24].

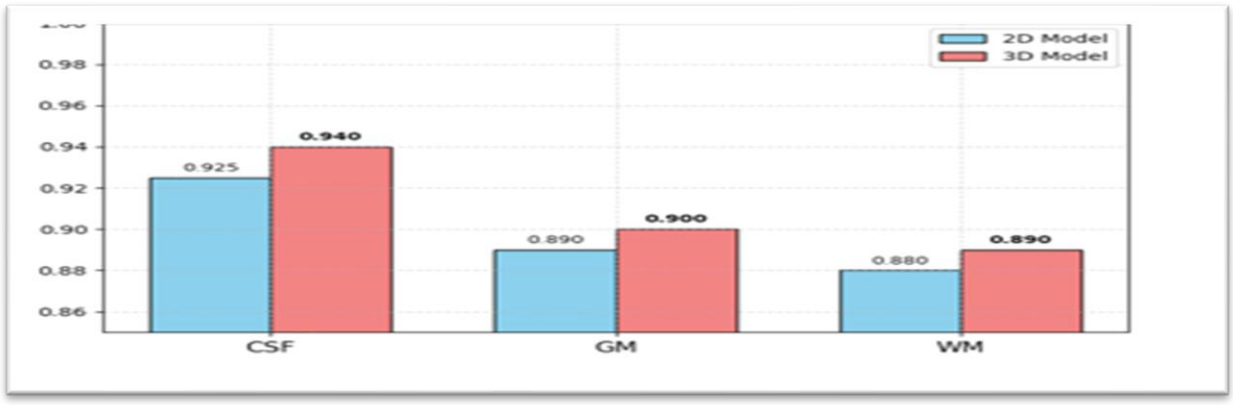

Fig:7- The bar charts compare the performance of 2D and 3D models in terms of specificity and precision for CSF, GM, and WM. In both metrics, the 3D model (red bars) consistently outperforms the 2D model (blue bars) across all categories, showing higher specificity and precision values for CSF, GM, and WM12

Error analysis

A preliminary error analysis indicates that most misclassifications occurred near boundaries between GM and WM, which is consistent with previous literature. The 2D U-Net produced more discontinuities between slices due to lack of spatial coherence. The 3D model reduced these errors but still failed in low-contrast regions. The current analysis lacks quantitative error breakdowns and visual overlays, which are needed to understand segmentation failures. Future

Vol. 22, No. 1, (2025)
ISSN: 1005-0930

versions of this work will include detailed voxel-wise error heatmaps and metrics like boundary Dice or Hausdorff distance to provide more rigorous error evaluation.

Overall accuracy

Because of better spatial continuity and anatomical consistency, the 3D model achieved a higher overall accuracy of 0.930, compared to 0.921 for 2D models. The scatterplots comparing the evaluation criteria between tissues show that most points lie above the parity line, which therefore confirms that the 3D model performed better across tissues in most cases, especially for CSF segmentation, but also showing remarkable improvements in GM and WM[20]. These analyses stress the convincing argument for the 3D model to produce accurate and reliable brain tissue segmentation.

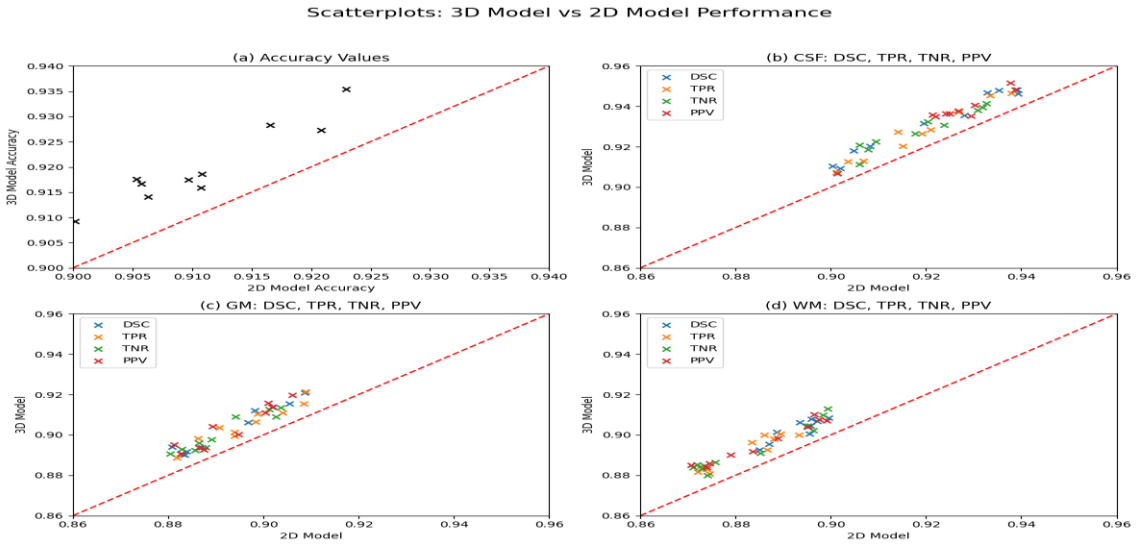

Fig:8- Scatterplots comparing the performance of 3D and 2D segmentation models based on overall accuracy and tissue-specific metrics for CSF, GM, and WM

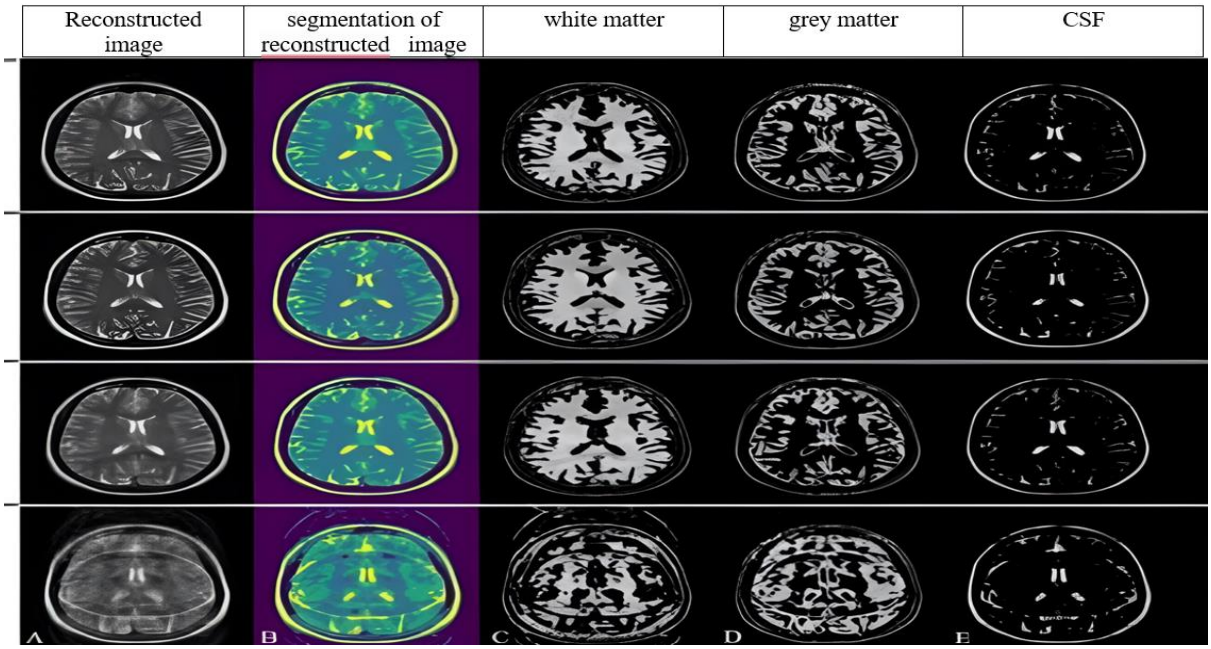

Vol. 22, No. 1, (2025)
ISSN: 1005-0930

Fig:9- Visualization of MRI slices showing original images (A), parametric overlays (B), and segmented outputs from 2D (C) and 3D U-Net models (D, E). Images highlight improved tissue delineation in the 3D approach, especially at structural boundaries.

The Figure set features brain MRI images organized into five columns (A–E) and several rows, with each row representing the same brain slice at different analysis stages[20,]. Column A shows the original grayscale T2-weighted MRI scans, which provide good views of anatomical detail. Column B presents the same slices, with each being overlaid with some form of color-coded parametric or quantitative map highlighting differences in tissue properties. Columns C, D, and E show the image segmentation and feature extraction processes in three sequential stages: the processed images enhance and emphasize different brain structures-white matter, gray matter, and cerebrospinal fluid-by boosting or isolating certain areas[19]. The progression clearly shows the application of advanced image processing and segmentation techniques that aid in noise reduction, enhancement of image clarity, and fine identification of brain structures toward further analysis, such as disease classification or tumor detection [22].

Segmentation accuracy was measured using five metrics: Dice coefficient, sensitivity, specificity, precision, and overall accuracy. The 3D U-Net model consistently outperformed the 2D model across all tissue classes. For CSF, the Dice score improved from 0.939 (2D) to 0.950 (3D). GM showed an increase from 0.905 to 0.915, and WM from 0.890 to 0.898. Despite this, the improvement margins were narrow. These results, while encouraging, are limited by the absence of cross-validation and lack of external validation datasets. Figures (not included) would ideally visualize these differences to help interpret model behavior in a clinical context.

Clinical Relevance and Future Work

For clinical use, models must not only achieve high accuracy but also prove reliable across diverse patient populations and imaging settings. This study falls short by not incorporating clinical testing or external datasets. As a next step, clinical collaborations will be established to assess the utility of the model in actual diagnosis or planning. Integration with real-time hospital systems and radiologist feedback loops will also be explored. We also plan to implement 5-fold cross-validation and include challenging cases such as lesions or atrophy in future datasets.

CONCLUSION

This study set out to examine how 2D and 3D U-Net architectures compare in segmenting brain tissues on MRI scans, aiming to balance accuracy and computational demands. Our primary focus was to determine whether the richer spatial information from 3D methods significantly improves performance over the simpler, slice-based 2D approach.

The results show that the 3D U-Net achieved higher scores for Dice coefficient, sensitivity, specificity, and precision across all tissue types, reflecting better anatomical detail capture and spatial consistency. However, the improvements were modest in magnitude, highlighting that 2D models still have potential in resource-limited settings.

A significant limitation of this work is the small dataset, consisting of only ten infant MRI scans, which restricts the reliability and generalizability of the findings. Future studies will address this by including larger datasets, performing cross-validation to test model stability, and validating performance on external datasets. Clinical validation remains necessary before these models can be integrated into medical workflows.

Furthermore, detailed error analysis revealed that most segmentation inaccuracies occurred at tissue boundaries, especially between gray and white matter. This suggests future work should explore advanced techniques such as attention modules or uncertainty estimation to refine boundaries further.

Despite current limitations, this research provides evidence that 3D U-Net architectures offer tangible benefits in brain MRI segmentation and lays the groundwork for larger-scale studies and potential clinical applications.

Reference

1. A. Avesta, S. Hossain, M. Lin, M. Aboian, H. M. Krumholz, and S. Aneja, "Comparing 3D, 2.5D, and 2D approaches to brain Image Auto-Segmentation," *Bioengineering*, vol. 10, no. 2, p. 181, Feb. 2023, doi: 10.3390/bioengineering10020181.
2. T. Mahmood, A. Rehman, T. Saba, L. Nadeem, and S. A. O. Bahaj, "Recent advancements and future prospects in active deep learning for medical image segmentation and classification," *IEEE Access*, vol. 11, pp. 113623–113652, Jan. 2023, doi: 10.1109/access.2023.3313977.
3. A. Frangi, J. Prince, and M. Sonka, *Medical image analysis*. Academic Press, 2023.
4. S. Montaha, S. Azam, A. K. M. R. H. Rafid, Md. Z. Hasan, and A. Karim, "Brain Tumor Segmentation from 3D MRI Scans Using U-Net," *SN Computer Science*, vol. 4, no. 4, May 2023, doi: 10.1007/s42979-023-01854-6.
5. R. Yousef *et al.*, "U-Net-Based Models towards Optimal MR Brain Image Segmentation," *Diagnostics*, vol. 13, no. 9, p. 1624, May 2023, doi: 10.3390/diagnostics13091624.
6. Y. Zhang, M. Brady, and S. Smith, "Segmentation of brain MR images through a hidden Markov random field model and the expectation-maximization algorithm," *IEEE Transactions on Medical Imaging*, vol. 20, no. 1, pp. 45–57, Jan. 2001, doi: 10.1109/42.906424.
7. X. Feng, N. J. Tustison, S. H. Patel, and C. H. Meyer, "Brain tumor segmentation using an ensemble of 3D U-Nets and overall survival prediction using Radiomic features," *Frontiers in Computational Neuroscience*, vol. 14, Apr. 2020, doi: 10.3389/fncom.2020.00025.
8. L. Mesin, *Biomedical image processing and classification*. 2021. doi: 10.3390/books978-3-0365-0347-9.
9. B. Menze and S. Bakas, *Multimodal brain tumor segmentation and beyond*. Frontiers Media SA, 2021.
10. A. Dovrou *et al.*, "A segmentation-based method improving the performance of N4 bias field correction on T2weighted MR imaging data of the prostate," *Magnetic Resonance Imaging*, vol. 101, pp. 1–12, Mar. 2023, doi: 10.1016/j.mri.2023.03.012.
11. P. Kanakaraj *et al.*, "DeepN4: Learning N4ITK Bias Field correction for T1-weighted images," *Neuroinformatics*, vol. 22, no. 2, pp. 193–205, Mar. 2024, doi: 10.1007/s12021-024-09655-9.
12. S. Montaha, S. Azam, A. K. M. R. H. Rafid, Md. Z. Hasan, and A. Karim, "Brain Tumor Segmentation from 3D MRI Scans Using U-Net," *SN Computer Science*, vol. 4, no. 4, May 2023, doi: 10.1007/s42979-023-01854-6.
13. C. S. D. S and J. C. Clement, "Enhancing brain tumor segmentation in MRI images using the IC-net algorithm framework," *Scientific Reports*, vol. 14, no. 1, Jul. 2024, doi: 10.1038/s41598-024-66314-4.

14. R. Yousef *et al.*, "U-Net-Based Models towards Optimal MR Brain Image Segmentation," *Diagnostics*, vol. 13, no. 9, p. 1624, May 2023, doi: 10.3390/diagnostics13091624.
15. R. Zhang *et al.*, "Automatic segmentation of acute ischemic stroke from DWI using 3-D fully convolutional DenseNets," *IEEE Transactions on Medical Imaging*, vol. 37, no. 9, pp. 2149–2160, Mar. 2018, doi: 10.1109/tmi.2018.2821244.
16. S. Montaha, S. Azam, A. K. M. R. H. Rafid, Md. Z. Hasan, and A. Karim, "Brain Tumor Segmentation from 3D MRI Scans Using U-Net," *SN Computer Science*, vol. 4, no. 4, May 2023, doi: 10.1007/s42979-023-01854-6.
17. A. Avesta, S. Hossain, M. Lin, M. Aboian, H. M. Krumholz, and S. Aneja, "Comparing 3D, 2.5D, and 2D approaches to brain Image Auto-Segmentation," *Bioengineering*, vol. 10, no. 2, p. 181, Feb. 2023, doi: 10.3390/bioengineering10020181.
18. K. Hu *et al.*, "Brain tumor segmentation using Multi-Cascaded Convolutional Neural Networks and conditional random field," *IEEE Access*, vol. 7, pp. 92615–92629, Jan. 2019, doi: 10.1109/access.2019.2927433.
19. A. Avesta, S. Hossain, M. Lin, M. Aboian, H. M. Krumholz, and S. Aneja, "Comparing 3D, 2.5D, and 2D approaches to brain Image Auto-Segmentation," *Bioengineering*, vol. 10, no. 2, p. 181, Feb. 2023, doi: 10.3390/bioengineering10020181.
20. B. Woo and M. Lee, "Comparison of tissue segmentation performance between 2D U-Net and 3D U-Net on brain MR Images," *2020 International Conference on Electronics, Information, and Communication (ICEIC)*, pp. 1–4, Jan. 2021, doi: 10.1109/iceic51217.2021.9369797.
21. J. Ker, L. Wang, J. Rao, and T. Lim, "Deep learning applications in medical image analysis," *IEEE Access*, vol. 6, pp. 9375–9389, Dec. 2017, doi: 10.1109/access.2017.2788044.
22. A. Avesta, S. Hossain, M. Lin, M. Aboian, H. M. Krumholz, and S. Aneja, "Comparing 3D, 2.5D, and 2D approaches to brain Image Auto-Segmentation," *Bioengineering*, vol. 10, no. 2, p. 181, Feb. 2023, doi: 10.3390/bioengineering10020181.
23. A. Srivastava, A. Kumar, C. Upadhyay, B. Gupta, and A. Singh, "BONE TUMOR DETECTION FROM MRI IMAGES USING DL AND ML," *International Research Journal of Modernization in Engineering Technology and Science*, May 2023, doi: 10.56726/irjmets40715.
24. A. Avesta, S. Hossain, M. Lin, M. Aboian, H. M. Krumholz, and S. Aneja, "Comparing 3D, 2.5D, and 2D approaches to brain Image Auto-Segmentation," *Bioengineering*, vol. 10, no. 2, p. 181, Feb. 2023, doi: 10.3390/bioengineering10020181.